

Published in final edited form as:

*Neuron*. 2014 February 5; 81(3): 536–543. doi:10.1016/j.neuron.2013.12.018.

## Axonal transport of TDP-43 mRNA granules in neurons is impaired by ALS-causing mutations

Nael H. Alami<sup>#1</sup>, Rebecca B. Smith<sup>#1</sup>, Monica A. Carrasco<sup>2</sup>, Luis A. Williams<sup>3</sup>, Christina S. Winborn<sup>4</sup>, Steve S. W. Han<sup>3,5</sup>, Evangelos Kiskinis<sup>3</sup>, Brett Winborn<sup>1</sup>, Brian D. Freibaum<sup>1</sup>, Anderson Kanagaraj<sup>1</sup>, Alison J. Clare<sup>1</sup>, Nisha M. Badders<sup>1</sup>, Bilada Bilican<sup>6</sup>, Edward Chaum<sup>4</sup>, Siddharthan Chandran<sup>6</sup>, Christopher E. Shaw<sup>7</sup>, Kevin C. Eggan<sup>3</sup>, Tom Maniatis<sup>2</sup>, and J. Paul Taylor<sup>1,\*</sup>

<sup>1</sup>Department of Developmental Neurobiology, St. Jude Children's Research Hospital, Memphis, Tennessee 38105, USA

<sup>2</sup>Department of Biochemistry and Molecular Biophysics, Columbia University Medical Center, New York, NY 10032, USA

<sup>3</sup>Department of Stem Cell and Regenerative Biology, Harvard University, Cambridge, MA 02138

<sup>4</sup>Department of Ophthalmology, University of Tennessee Health Sciences Center, Memphis, TN 38163, USA

<sup>5</sup>Department of Neurology, Massachusetts General Hospital, Boston, MA 02114, USA

<sup>6</sup>Euan MacDonald Centre for Motor Neurone Disease Research, Medical Research Council Centre for Regenerative Medicine, Centre for Neuroregeneration, University of Edinburgh, Edinburgh EH16 4SB, UK

<sup>7</sup>Departments of Clinical Neuroscience and Neurodegeneration and Brain Injury, King's College London and King's Health Partners, MRC Centre for Neurodegeneration Research, London SE5 8AF, UK

# These authors contributed equally to this work.

### Summary

The RNA binding protein TDP-43 regulates RNA metabolism at multiple levels, including transcription, RNA splicing, and mRNA stability. TDP-43 is a major component of the cytoplasmic inclusions characteristic of amyotrophic lateral sclerosis and some types of frontotemporal lobar degeneration. The importance of TDP-43 in disease is underscored by the fact that dominant missense mutations are sufficient to cause disease, although the role of TDP-43 in pathogenesis is unknown. Here we show that TDP-43 forms cytoplasmic mRNP granules that undergo bidirectional, microtubule-dependent transport in neurons *in vitro* and *in vivo* and facilitate delivery of target mRNA to distal neuronal compartments. TDP-43 mutations impair this mRNA transport function *in vivo* and *in vitro*, including in stem cell-derived motor neurons from ALS patients bearing any one of three different TDP-43 ALS-causing mutations. Thus, TDP43 mutations that cause ALS lead to partial loss of a novel cytoplasmic function of TDP-43.

© 2013 Elsevier Inc. All rights reserved.

\*Correspondence: jpaul.taylor@stjude.org.

**Publisher's Disclaimer:** This is a PDF file of an unedited manuscript that has been accepted for publication. As a service to our customers we are providing this early version of the manuscript. The manuscript will undergo copyediting, typesetting, and review of the resulting proof before it is published in its final citable form. Please note that during the production process errors may be discovered which could affect the content, and all legal disclaimers that apply to the journal pertain.

None of the authors of this manuscript have a financial interest related to this work.

## Introduction

Transactive response DNA-binding protein 43 (TDP-43) is a highly conserved, ubiquitously expressed heterogeneous ribonucleoprotein (hnRNP) that is primarily nuclear, but shuttles between the cytoplasm and nucleus. TDP-43 was initially identified as a transcription repressor (Ou et al., 1995) and splicing regulator (Buratti et al., 2001), but later recognized as the major component of pathological cytoplasmic inclusions characteristic of frontotemporal lobar degeneration (FTLD), amyotrophic lateral sclerosis (ALS), and inclusion body myopathy (Neumann et al., 2006; Salajegheh et al., 2009). Dominant mutations in TDP-43 are sufficient to cause familial forms of those diseases, underscoring its role in pathogenesis (Al-Chalabi et al., 2012). The identification of mutations in related RNA processing proteins has focused interest on perturbed RNA metabolism as a potential common defect underlying neurodegenerative diseases (Kim et al., 2013; Kwiatkowski et al., 2009; Lefebvre et al., 1995; Ramaswami et al., 2013), yet the role(s) of TDP-43 in RNA metabolism is far from complete. How disease-causing mutations disrupt TDP-43 function(s), the relative contribution of toxic gain vs. loss of function to disease, and the cellular compartment(s) in which this perturbation occurs, remains to be determined.

TDP-43 binds to thousands of mRNAs, many of which are important in brain development and synaptic function, but regulates alternative splicing of a small subset of these (Colombrita et al., 2012; Polymenidou et al., 2011; Tollervey et al., 2011; Xiao et al., 2011). Isolation of TDP-43 from a cytoplasmic fraction of human brain revealed binding to the 3'-UTR of numerous target mRNAs, suggesting a role in mRNA stability and/or transport (Tollervey et al., 2011). TDP-43 co-purifies with proteins involved in RNA transport (Freibaum et al., 2010), is trafficked in neurons (Fallini et al., 2012; Wang et al., 2008), and is detected in distal compartments such as the presynaptic membrane of axon terminals in the neuromuscular junction in mice (Narayanan et al., 2012). As such, it has been suggested that TDP-43 plays a role in the transport of certain target mRNAs into distal neuronal processes, but direct evidence is lacking (Lagier-Tourenne et al., 2010). The extent to which this hypothetical function might be compromised by disease mutations has not been explored.

### Axonal trafficking of TDP-43 granules in *Drosophila* motor neurons is impaired by ALS mutations

TDP-43 is highly conserved throughout the animal kingdom, and knockout of the gene encoding TDP-43 is lethal in mouse (Sephton et al., 2010). We used several model systems, including *Drosophila*, mouse, and human stem cell-derived motor neurons to systematically study TDP-43 function and the consequence of disease mutations. *Drosophila* that lack TBPH, the TDP-43 ortholog, typically die as pupae and escapers exhibit motor neuron synaptic dysfunction, progressive loss of motor neurons, and reduced life span (Diaper et al., 2013; Feiguin et al., 2009; Vanden†Broeck et al., 2013). This loss of function phenotype can be rescued by stably introducing wild-type human TDP-43 (TDP-43<sub>WT</sub>) illustrating conservation of TDP-43 function and validating *Drosophila* as a relevant model system (Fig. S1A). By contrast, introduction of TDP-43 harboring ALS-causing mutations (TDP-43<sub>M337V</sub>) at equivalent expression levels fails to rescue the motor neuron defect (Fig. S1A), suggesting that at least one consequence of disease-causing mutation is partial loss of function. To study TDP-43 in *Drosophila* in more detail we used PhiC31 integrase-mediated transgenesis to generate animals expressing equal levels of fluorescently tagged TDP-43<sub>WT</sub>, or either of the two ALS-causing mutants TDP-43<sub>M337V</sub> or TDP-43<sub>A315T</sub>, and monitored protein localization in motor neurons of animals with matched total expression levels (Fig. S1 G-H). The distribution of TDP-43<sub>WT</sub> was primarily nuclear as expected, (Fig. S1 B-C,

G), but we also observed numerous cytoplasmic granules along the length of axons and extending into the neuromuscular junction (NMJ), where TDP-43 fluorescence was diffuse (Fig. S1 G). By contrast, TDP-43<sub>M337V</sub> and TDP-43<sub>A315T</sub> accumulated in the cell soma and proximal axons (Fig. S1 B-D) but was absent or reduced at distal axons and the NMJ (Fig. S1 E-F). Live imaging of *Drosophila* motor neurons revealed that both wild-type (Movie S1) and mutant TDP-43 granules were transported bidirectionally for long distances with brief pauses (Fig. 1 A). We also observed that mutant TDP-43 granules were not transported efficiently along neuronal axons and displayed a less continuous movement that is evident when plotted using kymographs (Fig. 1A-F). The marked difference in subcellular distribution and transport behavior of wild-type and mutant TDP-43 prompted us to analyze the kinetics of TDP-43 transport in motor neurons. We observed a significant reduction in net anterograde displacement of TDP-43<sub>M337V</sub> and TDP-43<sub>A315T</sub> granules relative to TDP-43<sub>WT</sub> granules ( $p=0.027$  and  $0.018$  respectively; Fig. 1G, Table S1). Interestingly, we also observed that a greater fraction of TDP-43<sub>M337V</sub> and TDP-43<sub>A315T</sub> granules moved in the retrograde direction relative to TDP-43<sub>WT</sub> granules (Fig. 1I). These data suggest impaired anterograde movement of TDP-43<sub>M337V</sub> and TDP-43<sub>A315T</sub> granules along motor neuron axons *in vivo*, leading to mutant TDP-43 accumulation in the cytoplasm and proximal axons and deficiency at the NMJ.

### Axonal trafficking of TDP-43 granules in mouse cortical neurons is selectively impaired by ALS mutations

The presence of TDP-43 in cytoplasmic granules *in vivo* that are dynamic and transported along axons in *Drosophila*, prompted us to study the biology of these motile granules in primary mouse cortical neurons. Under normal conditions, endogenous TDP-43 was predominantly nuclear, as described previously (Barmada et al., 2010), though cytoplasmic puncta in neurites were also observed in most cells (Fig. S2A). Exogenous expression of mCherry-TDP-43<sub>WT</sub> showed the same distribution, and enabled live imaging of TDP-43 (Fig. S2B-C). Time-lapse imaging of mCherry-tagged TDP-43 granules in the axons of cortical neurons maintained in culture for 5 to 7 days revealed rapid, bidirectional, intermittent movement (Fig. 2A-B), consistent with the kinetics of TDP-43 granule transport observed in *Drosophila* motor neurons. The instantaneous velocities of TDP-43 granules *in vivo* and *in vitro* (Table S1) were consistent with microtubule-dependent fast axonal transport. TDP-43 granule movement was unaffected by treatment with latrunculin, which disrupts actin filaments, but abolished by treatment with nocodazole, which disrupts microtubules (Fig. 2C). This microtubule-dependent transport of TDP-43 granules is consistent with long-range axonal transport of protein complexes in neurons (Brown, 2013). To determine whether the ALS-causing mutations in TDP-43 influence granule trafficking, we compared trafficking parameters in neurons transfected with either mCherry-TDP-43<sub>WT</sub>, mCherry-TDP-43<sub>M337V</sub>, or mCherry-TDP-43<sub>A315T</sub>. Although the granule transport instantaneous velocities were indistinguishable, mCherry-TDP-43<sub>M337V</sub> and mCherry-TDP-43<sub>A315T</sub> granules were more frequently immotile ( $p=0.036$  and  $0.0027$ , respectively) and reversed direction significantly more frequently ( $p=0.0017$  and  $0.0032$ , respectively; Fig 2 D-E). These altered trafficking parameters of mutant TDP-43 granules were reflected in significant reductions in net displacement of TDP-43<sub>M337V</sub> and TDP-43<sub>A315T</sub> (TDP-43<sub>M337V</sub>:  $p<0.001$  in both directions; TDP-43<sub>A315T</sub>:  $p=0.030$  anterograde and  $0.045$  retrograde; Fig. 2F, Table S1). Interestingly, we observed a significant increase in retrograde movement of mutant TDP-43 granules as compared to wild-type (TDP-43<sub>M337V</sub>:  $p=0.037$ ; TDP-43<sub>A315T</sub>:  $p=0.042$ ; Fig. 2H).

To determine whether TDP-43 mutations result in generalized disruption of anterograde transport, we monitored mitochondrial trafficking and TDP-43 granule trafficking simultaneously in the same cells. In primary cortical neurons, axonal transport of

mitochondria was indistinguishable between cells expressing WT or mutant TDP-43 (M337V or A315T mutants) at 5-7 days in culture (Fig. 2G, I; Table S1) despite a significant defect in axonal transport of TDP-43 granules. We conclude that TDP-43 mutation results in a selective defect in the trafficking of TDP-43-containing granules, although this could lead to broader cellular toxicity and a more generalized defect in axonal transport in neurons cultured for longer periods of time (Wang et al., 2013).

### **TDP-43 is a component of trafficked mRNP granules and facilitates trafficking of cognate mRNA**

We and others have shown that TDP-43 interacts with a network of RNA-binding proteins (Fallini et al., 2012; Freibaum et al., 2010; Ling et al., 2010). The TDP-43 interactome includes numerous proteins involved in RNA trafficking, suggesting that some fraction of TDP-43 is a component of mRNP granules transported along neuronal axons. TDP-43 co-immunopurifies and colocalizes with the RNA trafficking protein Staufen (Fig. S3 A-B). Further, we determined that actively transported axonal TDP-43 granules stain positively with SYTO RNASelect Green fluorescent stain, consistent with the notion that TDP-43 granules transported along axons of cortical neurons contain RNA (Fig. S3C).

A limitation of SYTO RNASelect stain is that it is a non-specific, general RNA dye. To investigate the association of TDP-43 with one of its well-characterized mRNA targets, we designed a “mRNA beacon” consisting of a Cy3-tagged oligonucleotide that specifically hybridizes to mouse or human Neurofilament-L (*Nefl* or *NEFL*, respectively) mRNA and studied mRNA trafficking in live cells (Fig. 3A, Fig. S3 D-E). Neurofilament-L mRNA has a consensus TDP-43 binding site in its 3'-UTR and binds TDP-43 in extracts from human and mouse brain tissue (Polymenidou et al., 2011; Volkening et al., 2009). Fluorescence emission from the mRNA beacon is quenched until hybridization to *Nefl* mRNA and conjugation to a NeutrAvidin polypeptide prevents accumulation of beacon in the nucleus (Fig. 3A; Fig. S3E). Live-fluorescent imaging of mouse cortical neurons showed that *Nefl* mRNA is present throughout the axonal compartment and can be observed distally, even in the growth cones (Fig. 3B-C). *Nefl* mRNP granules moved bidirectionally along axons with intermittent rapid movements indistinguishable from those of TDP-43 granules (Fig. 3D, Movie S2). *Nefl* mRNP granules existed in two fractions: co-localized with fluorescently labeled TDP-43 (Fig. 3E) and those without any TDP-43 staining. Importantly, these two fractions showed different trafficking behavior. Specifically, *Nefl* mRNP granules that contained TDP-43 showed net anterograde movement, whereas those *Nefl* mRNP granules without TDP-43 showed net retrograde movement (Fig. 3F). We conclude that TDP-43 is specifically associated with mRNP granules that promote anterograde transport of certain mRNAs, is a marker of such granules, and could even participate in this process.

### **Defective trafficking of TDP-43 cognate mRNA in motor neurons derived from ALS patients with TDP-43 mutations**

The data derived from *Drosophila* motor neurons and mouse cortical neurons consistently show that TDP-43 granules undergo bidirectional transport and that this is selectively impaired by ALS-causing mutations in TDP-43. These data were generated by monitoring the trafficking of exogenous, fluorescently-tagged TDP-43. While this is standard in the trafficking field, there remains a possibility that over-expression of TDP-43 influences its behavior in these assays. The mRNA beacon we describe here, combined with recent advances in induced pluripotent stem (iPS) cell technology to generate motor neurons from ALS patients, affords a novel opportunity to corroborate our results in a relevant human cell type with endogenous wild-type or mutant TDP-43 expressed at physiological levels. Thus, we analyzed *NEFL* transport in iPS cell-derived human motor neurons carrying both of the ALS-causing mutations we analyzed in *Drosophila* and mouse cortical neurons (M337V and

A315T) and one additional ALS-causing mutation (G298S). The cells derived from an ALS patient with the M337V mutation were described previously (Bilican et al., 2012). These motor neurons exhibit increased cytoplasmic TDP-43 in the soma, accumulation of insoluble TDP-43 and accelerated cell death relative to control cells (Bilican et al., 2012). We monitored the movement of *NEFL* mRNA granules in axons of HB9-positive control or ALS motor neurons (TDP-43<sub>M337V</sub>; patient 31) in 3 time windows over 2 consecutive weeks following plating and prior to the observation of cell toxicity. *NEFL* mRNA granules underwent bidirectional, rapid movements that were interrupted by brief pauses in the axons of control and ALS motor neurons (Fig. 4B, Movie S3). The cells were monitored for a period of 2 weeks, after which it was not possible to clearly recognize individual axonal tracks extending from the cell soma to the growth cones without obstruction by glial cells or a significant decrease in the fluorescent intensity of the mRNA beacon. During the first week after plating, granule transport velocities, net displacement and directionality were indistinguishable between control and ALS motor neurons. By days 9-13, a defect in the transport of *NEFL* mRNA granules became apparent in ALS motor neurons. Specifically, anterograde transport of the *NEFL* mRNA granules significantly decreased (Fig. 4C). The frequency of reversals and the overall fraction of retrogradely moving granules also increased significantly in the ALS motor neurons ( $p=0.011$  and  $p=0.028$ , respectively), demonstrating less efficient transport mechanisms of *NEFL* mRNA (Fig. 4 C, E-F).

Given the inherent variability in motor neurons differentiated from human iPS cells, we generated additional control (Control line 2; patient 11 (Boulting et al., 2011)) and mutant iPS cell lines (TDP-43<sub>G298S</sub> and TDP-43<sub>A315T</sub>; patients 47 and RB20, respectively) (Fig. 4A, Fig S4). Examining these additional cell lines permitted us to determine whether impaired TDP-43 granule trafficking is solely a consequence of the M337V mutation or occurs more broadly with other TDP-43 mutations. In these cells, we monitored the movement of *NEFL* mRNA granules in 4 time windows over 17 days following plating. Our results again showed significant decrease in anterograde displacement that was quite profound ~10 days after plating and becomes progressively worse with time (Fig. 4D). We observe a significant increase in the frequency of reversals and retrograde movement of *NEFL* mRNA granules in iPS cell-derived motor neurons from ALS patients as compared to wild type after 9 days in culture (Fig. 4 D-E).

## Discussion

Here we establish that TDP-43 is a component of mRNA transport granules in neurons, including human stem cell-derived motor neurons, and identify a novel role for TDP-43 in the cytoplasm supporting anterograde axonal transport of target mRNAs from the soma to distal axonal compartments, including the NMJ. We also establish that three different ALS-causing mutations of TDP-43 impair this cytoplasmic function. This partial loss of function is consistent with the inability of mutant TDP-43 to complement a deficiency of endogenous *TBPH* in *Drosophila*. This transport defect is specific for TDP-43-positive mRNA granules, since another microtubule-dependent cargo in the same cells is transported normally during the same observation window. We conclude that deficient axonal transport of mRNA targeted by TDP-43 may contribute to pathogenesis of ALS and related diseases such as FTD.

Given the dominant inheritance of TDP-43 mutations in ALS, this defect in TDP-43 trafficking is unlikely to be the sole contribution of mutant TDP-43 to disease. Nevertheless, this clear and consistent defect in TDP-43 granule transport is likely an important contributor to ALS, perhaps influencing specific disease features such as cell type specificity or the pattern of degeneration. ALS has been described as a “distal axonopathy” because morphological abnormalities of the distal axon, including dismantling of the NMJ leading to

denervation, are among the earliest pathological features (Fischer et al., 2004). Many of the mRNA targets of TDP-43 encode proteins that function in this compartment but only a subset show differential splicing with altered TDP-43 levels or TDP-43 mutations (Arnold et al., 2013; Lagier-Tourenne et al., 2012; Polymenidou et al., 2011). One might speculate that a failure of TDP-43 to adequately support spatially appropriate translation of target mRNAs could contribute to this pattern of neurodegeneration.

The mechanism whereby disease-causing mutations impair granule transport is unclear, but could involve a defect in the ability of mutant TDP-43 granules to engage motor proteins or a physical impediment to their movement based on some abnormality in their size or shape. However, it is worth noting that these disease mutations all impact a prion-like domain in the C-terminus of TDP-43. Prion-like domains in TDP-43 and related RNA-binding proteins mediate the assembly of RNA granules, and disease mutations in these prion-like domains disturb the dynamics of RNA granule assembly and disassembly (Ramaswami et al., 2013). Normally, RNA transport granules in neurons are highly dynamic (Barbee et al., 2006) and this relates to their ability to deliver mRNAs to distal sites for local translation (Krichevsky and Kosik, 2001). The correlation between the impairment of RNA granule dynamics and impairment of RNA granule transport by ALS mutations suggests the possibility of a heretofore unappreciated role for RNA granule dynamism and transport that will require additional research to elucidate. The important take home messages from this study are that TDP-43 has a cytoplasmic function that is impaired by disease-causing mutations; TDP-43 is a component of neuronal RNA transport granules; association of target mRNAs with TDP-43 correlates with their anterograde transport; and ALS-causing mutations in TDP-43 impair this transport *in vivo* in *Drosophila*, in mouse cortical neurons, and in iPS-derived motor neurons from ALS patients.

## Experimental Procedures

### Drosophila

3<sup>rd</sup> instar *Drosophila* larvae genotypes OK371>Gal4/ UAS-Venus-TDP-43 WT, OK371>Gal4/ UAS-Venus-TDP-43 M337V, and OK371>Gal4/UAS-YFP-TDP-43 A315T were used for axonal transport imaging. For TDP-43 quantification at the cell body and synaptic terminal, UAS-CD8-RFP (Bloomington Stock Center, Indiana U, Bloomington, IN; stock #27391) was co-expressed, resulting in the genotypes: OK371>Gal4, UAS-CD8-RFP/ UAS-TDP-43 WT or OK371>Gal4, UAS-CD8-RFP/ UAS-TDP-43 M337V, OK371>Gal4, UAS-CD8-RFP/UAS-TDP-43 A315T, and negative control- OK371>Gal4, UAS-CD8-RFP/ +. OK371-Gal4 driver was used for all *Drosophila* transgene expression except for the TBPH rescue cross where Armadillo Gal4 was used. In TBPH viability rescue cross, transgenes (UAS-Venus-TBPH, UAS-Venus-TDP-43, and UAS-Venus-TDP43 M337V) were expressed by Armadillo Gal4 in TBPH  $\Delta$ 23 homozygote mutants. Controls in this analysis included W1118, homozygotes and heterozygotes for the null TBPH  $\Delta$ 23 mutation. Third instar larvae were sorted by genotype and placed in separate vials. The percentage of larvae that became living adults was recorded and graphed.

### Mouse primary neuron culture and transfection

Primary mouse cortical neuron culture and transfection were conducted as previously described (Kaech and Banker, 2006). Details are provided in supplemental methods.

### Confocal imaging

Imaging cortical neurons was done 5-8 days after plating, and human motor neurons 2-17 days after plating. For *in vivo* live imaging, wandering 3<sup>rd</sup> instar *Drosophila* larvae were dissected live in HL3 medium (Stewart et al., 1994); pinned to Sylgard in an imaging

chamber; eviscerated keeping CNS, nerves and muscle intact; and covered with a coverslip. Time-lapse movies were obtained using a spinning disc confocal Marianas system (Intelligent Imaging Innovations, Denver, CO) configured on a Zeiss Axio Observer. Further details can be found in supplemental methods.

### Image and movie analysis

In live *Drosophila* larvae samples, images of the NMJ at muscle 13 were examined for levels of Venus-TDP-43 fluorescence. Time-lapse movies were analyzed using SlideBook 5.5 or Imaris 7.6 (Bitplane Science Software, South Windsor, CT) with the manual particle-tracking module. Granules that moved  $>3 \mu\text{m}$  during the length of the movie were analyzed. In mouse cortical neurons, when granules changed direction, they were considered a new particle. However, in the moving vs. stationary analysis, granules changing direction were counted as 1 moving particle.

### Imaging mitochondrial transport

For live-cell imaging of mitochondria, cells transfected with fluorescent TDP-43 (wild-type or mutant) were incubated for 20 min in imaging media containing either Mitotracker Red FM (25 nM; Invitrogen), or Mitotracker Green FM (20 nM; Invitrogen). The cells were then imaged using live fluorescent confocal microscopy as described above.

### Co-immunoprecipitation

FLAG-tagged expression plasmids were transfected into HEK293T cells using Fugene 6 as recommended by manufacturer. Mock-transfected cells were used as negative control, and a 10 cm plate was used for each co-immunoprecipitation. 48 hrs later, cells were lysed and lysates were cleared by centrifugation at 21,000g. Clarified lysates were pre-cleared with normal mouse IgG agarose and protein G agarose prior to co-immunoprecipitation with anti-FLAG (M2, Sigma) agarose. Beads were washed and immunopurified proteins were eluted with FLAG peptide (Sigma). Proteins were separated by SDS-PAGE prior to protein identification by mass spectrometry. Where indicated, 45 $\mu\text{g}$  RNase A was added to each lysate prior to co-immunoprecipitation.

### Western blotting

To study the interaction between Stau1 and TDP-43, samples were separated by SDS-PAGE using AnyKD tris-glycine gels (Bio-Rad) and transferred to PVDF membrane. To detect expression levels of TDP-43, 3 *Drosophila* 3<sup>rd</sup> instar larvae brains were collected, homogenized, and reduced per lane. These samples were separated by SDS-PAGE using Novex NuPAGE Bis-Tris (Life Technologies) gels. Anti-TDP43 (Santa Cruz, sc-100871) and anti-STAU1 (ProteinTech, 14225-1-AP) were used.

### mRNA beacon design, synthesis, and testing

Beacon loop sequences of 23-25nt were designed manually to detect the mouse or human NFL transcript using 3 different programs in parallel; 1) OLIGOWALK, 2) mFold, and 3) MicroInspector. Using this approach, beacons were predicted to stably hybridize to single stranded regions of the transcript in areas not bound by endogenous microRNAs (Bratu et al., 2003; Rusinov et al., 2005). Beacons were synthesized using a nuclease resistant 2'-O-methylribonucleotide backbone and were prevented from nuclear localization by conjugation to NeutrAvidin (Chen et al., 2009; Chen et al., 2010). Beacons were synthesized with a biotin-modified-dT nucleotide in the 3' stem sequence and were labeled with 5' Cy3 and 3' BHQ2 by Sigma Aldrich (St. Louis, MO). The beacon sequences are: *Nefl* 5' - Cy3 GCTCAATCTTTCTTCTTAGCCACC(Bio-dt)gagc BHQ2-3', NEFL 5' - Cy3 cacaGGTTCAATCTTTCTTCTTAGCTGC(Bio-dT)gtg BHQ2 -3'. Underlined sequences

form the self-hybridizing stem sequence and upper case letters hybridize to the transcript. *Nefl* beacon hybridization to its target sequence was tested *in vitro* using synthetic oligonucleotides in solution. *Nefl* beacon hybridized rapidly with its target and high specific fluorescence was detected. Further details are provided in supplemental material.

### Generation and characterization of novel TDP-43 iPS cell lines

Novel iPS cell lines were characterized in this study: TDP-43<sub>A315T</sub> and TDP-43<sub>G298S</sub>. Dermal biopsies were obtained from 2 familial ALS patients with mutations in the *TARDBP* locus. From these explants, fibroblasts were generated and expanded in KO-DMEM (Life Technologies™) supplemented with 10% FBS (Hyclone™). TDP-43 iPS cells were derived by transduction of fibroblasts with retroviruses expressing *OCT4*, *SOX2* and *KLF4*. After 3-4 weeks, primary iPS cell colonies were picked based on morphology and independently expanded in mTeSR™1 medium (STEMCELL Technologies) to generate 4-6 different iPS cell lines/patient. The presence of the mutations was confirmed by PCR amplification of a genomic region surrounding *Exon 6*, followed by Sanger DNA sequencing. The pluripotency of the iPS cell lines used was validated using the TaqMan® hPSC Scorecard™ Panel (Life Technologies™). Expression of transcription factors and cell surface antigens characteristic of the pluripotent state was confirmed using immunocytochemistry. Primary antibodies and dilution factors used for this purpose were NANOG (1:100, R&D), OCT3/4 (1:500, Santa Cruz), SSEA-4 (1:1000, Santa Cruz) and TRA-1-81 (1:1000, Millipore).

### iPS and derived iPS motor neurons

Detailed description can be found in the Supplemental Materials section. Briefly, iPS cells were maintained on a monolayer of neomycin selected mouse embryonic fibroblasts (MEFs; Millipore) in hiPS media (Bilican et al., 2012; Dimos et al., 2008). To generate motor neurons, undifferentiated iPS cells were incubated with 10 μM Y27632 (Calbiochem) then passaged, triturated, and placed into ultra-low adherent culture dishes (Corning) for seeding of embryoid bodies (EBs). For the first 11 days, cells were kept in suspension in hiPS media without bFGF. At day 11, EBs were switched to neural induction medium. At day 28, EBs were dissociated, transfected using Lonza Nucleofector with mRNA beacons and HB9 (9Kb)-promoter-GFP, and plated onto PDL/laminin-coated (BD Biosciences) glass (Kaech and Banker, 2006). To prepare the cells for live imaging, cells were allowed to settle on glass coverslips flipped over primary glial monolayers.

### Statistical Analyses

Statistical analyses were performed with Prism6 (GraphPad Software Inc., La Jolla, CA). Comparing the TDP-43 wild-type to TDP-43 (M337V) datasets yielded all p-values. A Mann-Whitney unpaired test with one-tailed p-value was completed for comparing distances travelled, velocity analysis, and the directional percentages of granules within populations. A One-Way Anova test followed by a Tukey test was completed for the TBPH rescue analysis. KaleidaGraph (Synergy software) was used to make the axonal particle trafficking distance and velocity bar graphs. All error bars are shown as mean ± SEM.

### Supplementary Material

Refer to Web version on PubMed Central for supplementary material.

### Acknowledgments

We thank H. Mitsumoto and C. Henderson (Projet ALS/Columbia), and R. Brown (UMass Medical School) for collection of Patient 47 and Patient RB20 material. We also thank D. Zarnescu for providing the UAS-YFP-TDP-43(A315T) *Drosophila* lines and C. Gu and D. Solecki for provision of YFP-EB1 and pCIG2-GFP expression



plasmids, respectively. This work was supported by grants from the Packard Foundation, Muscular Dystrophy Association, the ALS Association, and NIH grants NS053825 and AG031587 to J.P.T., and an NIH Director's Pioneer Award to T.M. (8DP1NS082099). Images were acquired in the Cell & Tissue Imaging Center at St. Jude, which is supported by the American-Lebanese-Syrian Associated Charities and NCI P30 CA021765-34.

## Reference

- Al-Chalabi A, Jones A, Troakes C, King A, Al-Sarraj S, van den Berg LH. The genetics and neuropathology of amyotrophic lateral sclerosis. *Acta neuropathologica*. 2012; 124:339–352. [PubMed: 22903397]
- Arnold ES, Ling SC, Huelga SC, Lagier-Tourenne C, Polymenidou M, Ditsworth D, Kordasiewicz HB, McAlonis-Downes M, Platoshyn O, Parone PA, et al. ALS-linked TDP-43 mutations produce aberrant RNA splicing and adult-onset motor neuron disease without aggregation or loss of nuclear TDP-43. *Proc Natl Acad Sci U S A*. 2013; 110:E736–745. [PubMed: 23382207]
- Barbee SA, Estes PS, Cziko AM, Hillebrand J, Luedeman RA, Collier JM, Johnson N, Howlett IC, Geng C, Ueda R, et al. Staufen-and FMRP-containing neuronal RNPs are structurally and functionally related to somatic P bodies. *Neuron*. 2006; 52:997–1009. [PubMed: 17178403]
- Barmada SJ, Skibinski G, Korb E, Rao EJ, Wu JY, Finkbeiner S. Cytoplasmic mislocalization of TDP-43 is toxic to neurons and enhanced by a mutation associated with familial amyotrophic lateral sclerosis. *J Neurosci*. 2010; 30:639–649. [PubMed: 20071528]
- Bilican B, Serio A, Barmada SJ, Nishimura AL, Sullivan GJ, Carrasco M, Phatnani HP, Puddifoot CA, Story D, Fletcher J, et al. Mutant induced pluripotent stem cell lines recapitulate aspects of TDP-43 proteinopathies and reveal cell-specific vulnerability. *Proc Natl Acad Sci U S A*. 2012; 109:5803–5808. [PubMed: 22451909]
- Boulting GL, Kiskinis E, Croft GF, Amoroso MW, Oakley DH, Wainger BJ, Williams DJ, Kahler DJ, Yamaki M, Davidow L, et al. A functionally characterized test set of human induced pluripotent stem cells. *Nat Biotechnol*. 2011; 29:279–286. [PubMed: 21293464]
- Bratu DP, Cha BJ, Mhlanga MM, Kramer FR, Tyagi S. Visualizing the distribution and transport of mRNAs in living cells. *Proc Natl Acad Sci U S A*. 2003; 100:13308–13313. [PubMed: 14583593]
- Brown, A. Axonal Transport.. In: Pfaff, DW., editor. *Neuroscience in the 21st Century*. Springer; New York: 2013. p. 255-308.
- Buratti E, Dork T, Zuccato E, Pagani F, Romano M, Baralle FE. Nuclear factor TDP-43 and SR proteins promote in vitro and in vivo CFTR exon 9 skipping. *EMBO J*. 2001; 20:1774–1784. [PubMed: 11285240]
- Chen AK, Behlke MA, Tsourkas A. Sub-cellular trafficking and functionality of 2'-O-methyl and 2'-O-methyl-phosphorothioate molecular beacons. *Nucleic Acids Res*. 2009; 37:e149. [PubMed: 19820111]
- Chen AK, Davydenko O, Behlke MA, Tsourkas A. Ratiometric bimolecular beacons for the sensitive detection of RNA in single living cells. *Nucleic Acids Res*. 2010; 38:e148. [PubMed: 20507905]
- Colombrita C, Onesto E, Megiorni F, Pizzuti A, Baralle FE, Buratti E, Silani V, Ratti A. TDP-43 and FUS RNA-binding proteins bind distinct sets of cytoplasmic messenger RNAs and differently regulate their post-transcriptional fate in motoneuron-like cells. *J Biol Chem*. 2012
- Diaper DC, Adachi Y, Sutcliffe B, Humphrey DM, Elliott CJ, Stepto A, Ludlow ZN, Broeck LV, Callaerts P, Dermaut B, et al. Loss and gain of Drosophila TDP-43 impair synaptic efficacy and motor control leading to age-related neurodegeneration by loss-of-function phenotypes. *Hum Mol Genet*. 2013
- Dimos JT, Rodolfa KT, Niakan KK, Weisenthal LM, Mitsumoto H, Chung W, Croft GF, Saphier G, Leibel R, Golland R, et al. Induced pluripotent stem cells generated from patients with ALS can be differentiated into motor neurons. *Science*. 2008; 321:1218–1221. [PubMed: 18669821]
- Fallini C, Bassell GJ, Rossoll W. The ALS disease protein TDP-43 is actively transported in motor neuron axons and regulates axon outgrowth. *Hum Mol Genet*. 2012; 21:3703–3718. [PubMed: 22641816]
- Feiguin F, Godena VK, Romano G, D'Ambrogio A, Klima R, Baralle FE. Depletion of TDP-43 affects Drosophila motoneurons terminal synapsis and locomotive behavior. *FEBS Lett*. 2009; 583:1586–1592. [PubMed: 19379745]

- Fischer LR, Culver DG, Tennant P, Davis AA, Wang M, Castellano-Sanchez A, Khan J, Polak MA, Glass JD. Amyotrophic lateral sclerosis is a distal axonopathy: evidence in mice and man. *Exp Neurol*. 2004; 185:232–240. [PubMed: 14736504]
- Freibaum BD, Chitta RK, High AA, Taylor JP. Global analysis of TDP-43 interacting proteins reveals strong association with RNA splicing and translation machinery. *J Proteome Res*. 2010; 9:1104–1120. [PubMed: 20020773]
- Kaech S, Banker G. Culturing hippocampal neurons. *Nat Protoc*. 2006; 1:2406–2415. [PubMed: 17406484]
- Kim HJ, Kim NC, Wang YD, Scarborough EA, Moore J, Diaz Z, MacLea KS, Freibaum B, Li S, Molliex A, et al. Mutations in prion-like domains in hnRNPA2B1 and hnRNPA1 cause multisystem proteinopathy and ALS. *Nature*. 2013; 495:467–473. [PubMed: 23455423]
- Krichevsky AM, Kosik KS. Neuronal RNA granules: a link between RNA localization and stimulation-dependent translation. *Neuron*. 2001; 32:683–696. [PubMed: 11719208]
- Kwiatkowski TJ Jr, Bosco DA, Leclerc AL, Tamrazian E, Vanderburg CR, Russ C, Davis A, Gilchrist J, Kasarskis EJ, Munsat T, et al. Mutations in the FUS/TLS gene on chromosome 16 cause familial amyotrophic lateral sclerosis. *Science*. 2009; 323:1205–1208. [PubMed: 19251627]
- Lagier-Tourenne C, Polymenidou M, Cleveland DW. TDP-43 and FUS/TLS: emerging roles in RNA processing and neurodegeneration. *Human molecular genetics*. 2010
- Lagier-Tourenne C, Polymenidou M, Hutt KR, Vu AQ, Baughn M, Huelga SC, Clutario KM, Ling SC, Liang TY, Mazur C, et al. Divergent roles of ALS-linked proteins FUS/TLS and TDP-43 intersect in processing long pre-mRNAs. *Nat Neurosci*. 2012; 15:1488–1497. [PubMed: 23023293]
- Lefebvre S, Burglen L, Reboullet S, Clermont O, Bulet P, Viollet L, Benichou B, Cruaud C, Millasseau P, Zeviani M, et al. Identification and characterization of a spinal muscular atrophy-determining gene. *Cell*. 1995; 80:155–165. [PubMed: 7813012]
- Ling SC, Albuquerque CP, Han JS, Lagier-Tourenne C, Tokunaga S, Zhou H, Cleveland DW. ALS-associated mutations in TDP-43 increase its stability and promote TDP-43 complexes with FUS/TLS. *Proc Natl Acad Sci U S A*. 2010; 107:13318–13323. [PubMed: 20624952]
- Narayanan RK, Mangelsdorf M, Panwar A, Butler TJ, Noakes PG, Wallace RH. Identification of RNA bound to the TDP-43 ribonucleoprotein complex in the adult mouse brain. *Amyotroph Lateral Scler Frontotemporal Degener*. 2012
- Neumann M, Sampathu DM, Kwong LK, Truax AC, Micsenyi MC, Chou TT, Bruce J, Schuck T, Grossman M, Clark CM, et al. Ubiquitinated TDP-43 in frontotemporal lobar degeneration and amyotrophic lateral sclerosis. *Science*. 2006; 314:130–133. [PubMed: 17023659]
- Ou SH, Wu F, Harrich D, García-Martínez LF, Gaynor RB. Cloning and characterization of a novel cellular protein, TDP-43, that binds to human immunodeficiency virus type 1 TAR DNA sequence motifs. *J Virol*. 1995; 69:3584–3596. [PubMed: 7745706]
- Polymenidou M, Lagier-Tourenne C, Hutt KR, Huelga SC, Moran J, Liang TY, Ling S-C, Sun E, Wancewicz E, Mazur C, et al. Long pre-mRNA depletion and RNA missplicing contribute to neuronal vulnerability from loss of TDP-43. *Nat Neurosci*. 2011; 14:459–468. [PubMed: 21358643]
- Ramaswami M, Taylor JP, Parker R. Altered Ribostasis: RNA-Protein Granules in Degenerative Disorders. *Cell*. 2013; 154:727–736. [PubMed: 23953108]
- Rusinov V, Baev V, Minkov IN, Tabler M. MicroInspector: a web tool for detection of miRNA binding sites in an RNA sequence. *Nucleic Acids Res*. 2005; 33:W696–700. [PubMed: 15980566]
- Salajegheh M, Pinkus JL, Taylor JP, Amato AA, Nazareno R, Baloh RH, Greenberg SA. Sarcoplasmic redistribution of nuclear TDP-43 in inclusion body myositis. *Muscle & nerve*. 2009; 40:19–31. [PubMed: 19533646]
- Septon CF, Good SK, Atkin S, Dewey CM, Mayer P 3rd, Herz J, Yu G. TDP-43 is a developmentally regulated protein essential for early embryonic development. *J Biol Chem*. 2010; 285:6826–6834. [PubMed: 20040602]
- Stewart B, Atwood H, Renger J, Wang J, Wu C. Improved stability of *Drosophila* larval neuromuscular preparations in haemolymph-like physiological solutions. *J Comp Physiol*. 1994; 175:179–191.

- Tollervey JR, Curk T, Rogelj B, Briese M, Cereda M, Kayikci M, Konig J, Hortobagyi T, Nishimura AL, Zupunski V, et al. Characterizing the RNA targets and position-dependent splicing regulation by TDP-43. *Nat Neurosci.* 2011; 14:452–458. [PubMed: 21358640]
- Vandenbroeck L, Naval-Sanchez M, Adachi Y, Diaper D, Dourlen P, Chapuis J, Kleinberger G, Gistelinc M, Vandenbroeckhoven C, Lambert J-C, et al. TDP-43 Loss-of-Function Causes Neuronal Loss Due to Defective Steroid Receptor-Mediated Gene Program Switching in *Drosophila*. *Cell Reports.* 2013
- Volkening K, Leystra-Lantz C, Yang W, Jaffee H, Strong MJ. Tar DNA binding protein of 43 kDa (TDP-43), 14-3-3 proteins and copper/zinc superoxide dismutase (SOD1) interact to modulate NFL mRNA stability. Implications for altered RNA processing in amyotrophic lateral sclerosis (ALS). *Brain Res.* 2009; 1305:168–182. [PubMed: 19815002]
- Wang IF, Wu LS, Chang HY, Shen CK. TDP-43, the signature protein of FTL-D-U, is a neuronal activity-responsive factor. *J Neurochem.* 2008; 105:797–806. [PubMed: 18088371]
- Wang W, Li L, Lin WL, Dickson DW, Petrucelli L, Zhang T, Wang X. The ALS disease-associated mutant TDP-43 impairs mitochondrial dynamics and function in motor neurons. *Hum Mol Genet.* 2013
- Xiao S, Sanelli T, Dib S, Sheps D, Findlater J, Bilbao J, Keith J, Zinman L, Rogaeva E, Robertson J. RNA targets of TDP-43 identified by UV-CLIP are deregulated in ALS. *Mol Cell Neurosci.* 2011; 47:167–180. [PubMed: 21421050]

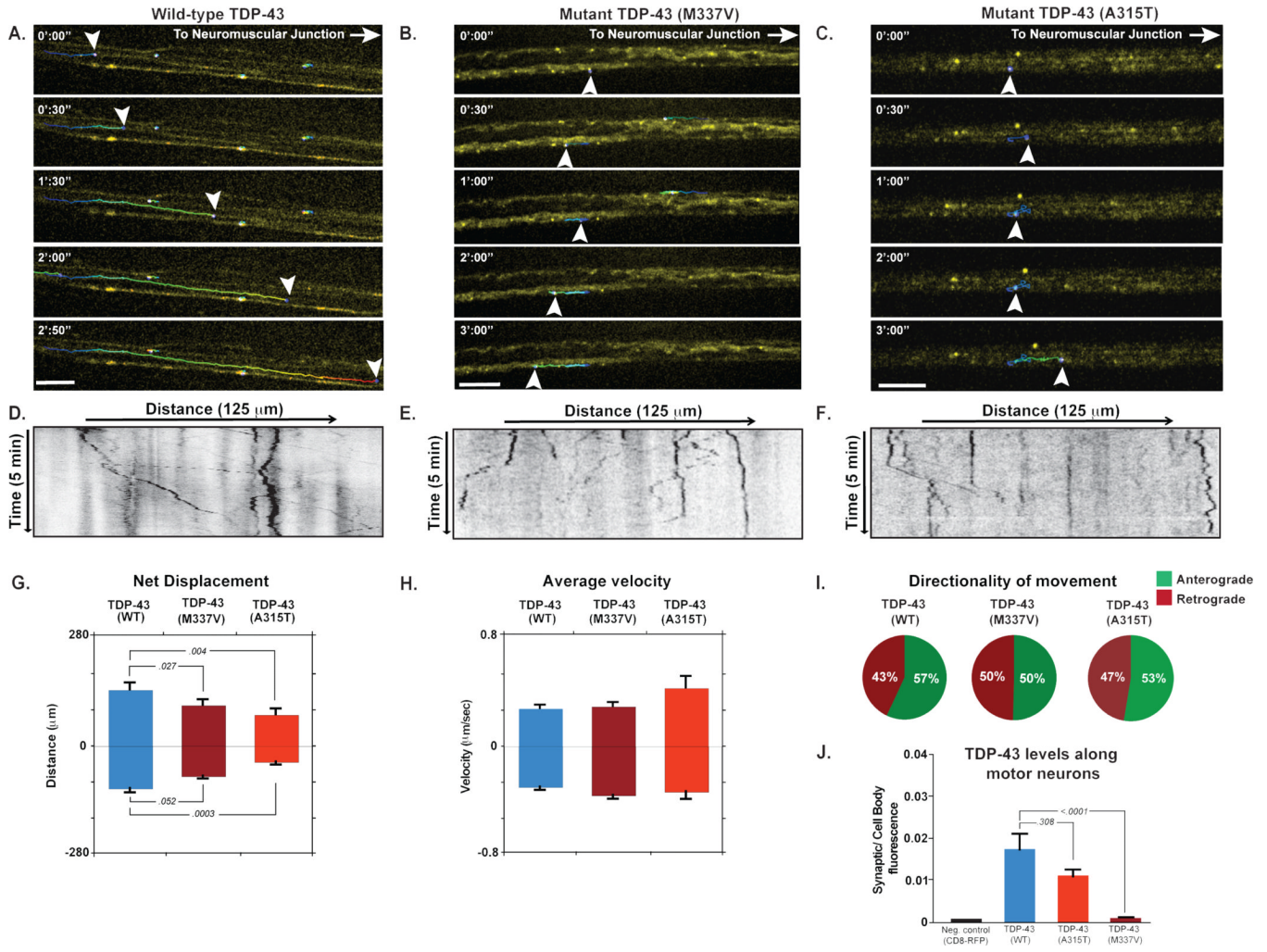


**Fig. 1. Localization and transport kinetics of TDP-43 granules in *Drosophila* motor neurons** (A-C) Venus-TDP-43<sub>WT</sub>, Venus-TDP-43<sub>M337V</sub>, and Venus-TDP-43<sub>A315T</sub> granules (arrowheads) displayed dynamic bidirectional movement along motor neuron axons of 3<sup>rd</sup> instar larvae. Transport of mutant TDP-43 granules showed normal instantaneous velocities, but an increased frequency of reversals and diminished net anterograde movement. Scale bar: 10 µm. (D-F) Kymographs tracing TDP-43 granules in motor neuron axons. (G-E) Quantification of displacement and instantaneous velocities of wild type and mutant granules along *Drosophila* motor neuron axons. Anterograde and retrograde movements are represented as positive or negative values on the y-axis, respectively. (I) Analysis of movement directionality shows a reduced ratio of anterograde to retrograde movement for mutant TDP-43 granules as compared to TDP-43<sub>WT</sub>. (J) Quantification of fluorescence intensities in *Drosophila* motor neuron axons. The ratio of average fluorescence intensity per pixel at the synaptic terminal divided by the fluorescence at the cell body shows that Venus-TDP-43<sub>WT</sub> signal is higher than that of mutant TDP-43. Error bars are shown as mean ± SEM.

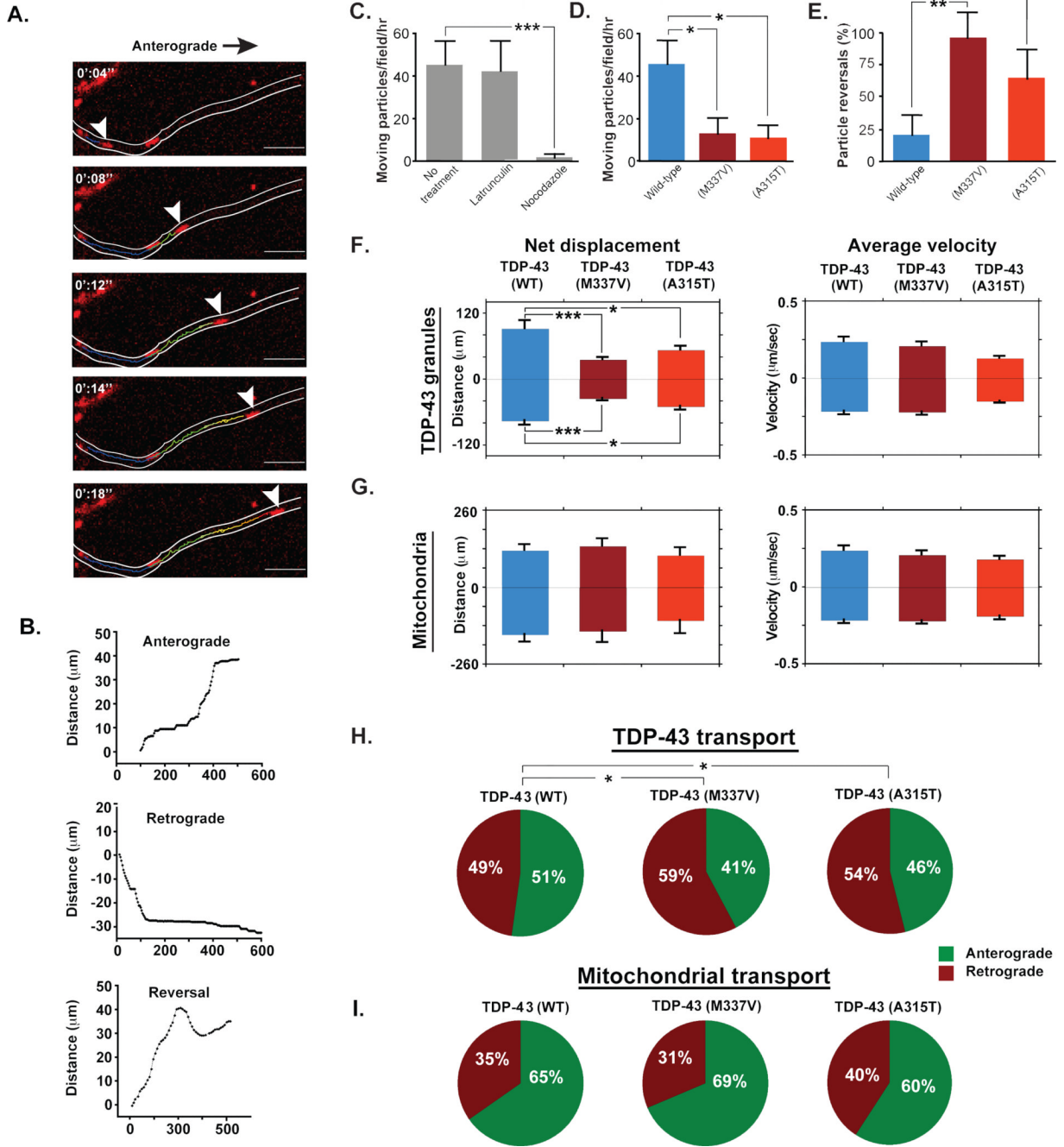


**Fig. 2. TDP-43 transport in primary cortical neurons**

(A) A wild-type TDP-43 granule (arrowhead) moves along the axon of mouse cortical neuron in the anterograde direction. Scale bar: 10  $\mu\text{m}$ . (B) 3 representative tracings of TDP-43 granules moving along the axons of cortical neurons illustrating anterograde displacement, retrograde displacement, and reversal of directionality. The x-axis represents time and the y-axis total distance along the axon. (C) The number of moving TDP-43 granules in wild type and mutant-transfected cells were normalized to movements per hour and plotted. Latrunculin treatment had no effect on TDP-43 transport, while nocodazole-treated cells contained dramatically fewer motile TDP-43 granules, demonstrating microtubule-dependent movement. (D) The fraction of motile mutant TDP-43 granules was

significantly reduced compared to TDP-43<sub>WT</sub> granules. (E) Mutant TDP-43 granules reversed direction significantly more frequently than TDP-43<sub>WT</sub> granules. (F) Kinetics of wild-type and mutant TDP-43 transport show a significant decrease in net displacement of TDP-43<sub>M337V</sub> ( $p < 0.001$ ) and TDP-43<sub>A315T</sub> ( $p = 0.030$  for anterograde and  $0.045$  for retrograde) as compared to TDP-43<sub>WT</sub>, and no significant change in instantaneous velocities. (G) Kinetics of mitochondrial transport show that there is no significant difference in mitochondrial transport in cells transfected with wild-type or mutant TDP-43. (H) The direction of transport of TDP-43 granules was altered in cells transfected with mutant TDP-43. A significantly higher percentage of TDP-43<sub>M337V</sub> and TDP-43<sub>A315T</sub> granules moved in the retrograde direction as compared to TDP-43<sub>WT</sub> granules ( $p = 0.037$  and  $0.042$ , respectively). (I) The direction of mitochondrial transport was not altered in cells transfected with wild-type or mutant TDP-43. All error bars are shown as mean  $\pm$  SEM.

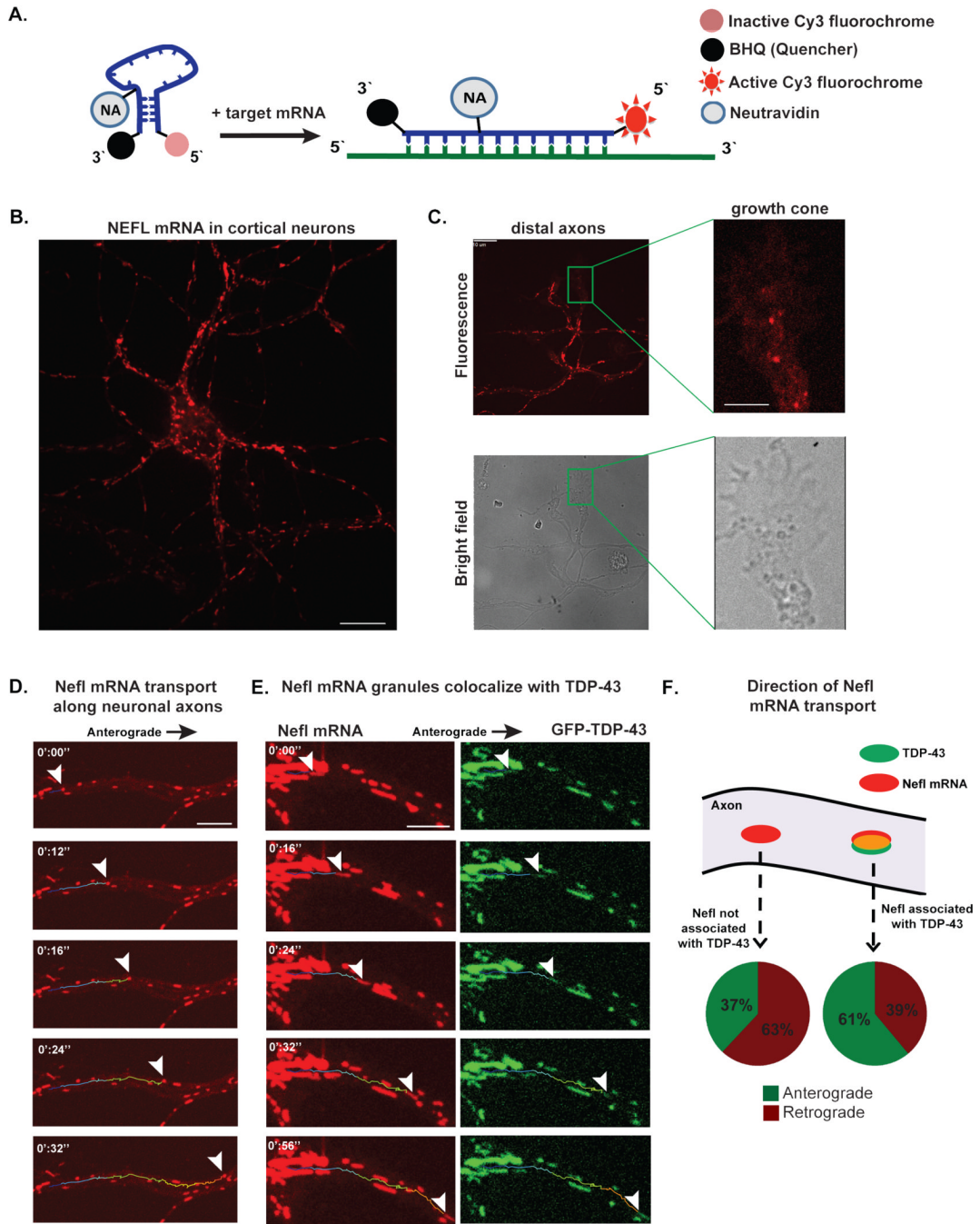


**Fig. 3. Nefl mRNA is transported bidirectionally along primary cortical neuron axons and is part of an mRNP granule that contains TDP-43**

(A) mRNA beacons are designed to target Nefl mRNA. The beacon emits a fluorescence signal once it linearizes upon hybridization with its target mRNA. (B) Nefl mRNA fluorescence is present in the soma and along primary cortical neuron axons. Scale bar: 10  $\mu\text{m}$ . (C) Nefl mRNA was detected in distal axonal compartments and inside growth cones. Scale bar: axons 10  $\mu\text{m}$ ; growth cone 2  $\mu\text{m}$ . (D) Nefl mRNA granule (arrowheads) is transported along the axon of a cortical neuron. Scale bar: 5  $\mu\text{m}$ . (E) TDP-43 is present in the motile mRNA granule in a cortical neuron. Scale bar: 10  $\mu\text{m}$ . (F) Granules containing TDP-43 and Nefl mRNA show predominately anterograde movements and net anterograde

displacement, whereas those that contain Nefl without TDP-43 show predominately retrograde movements and net retrograde displacement.



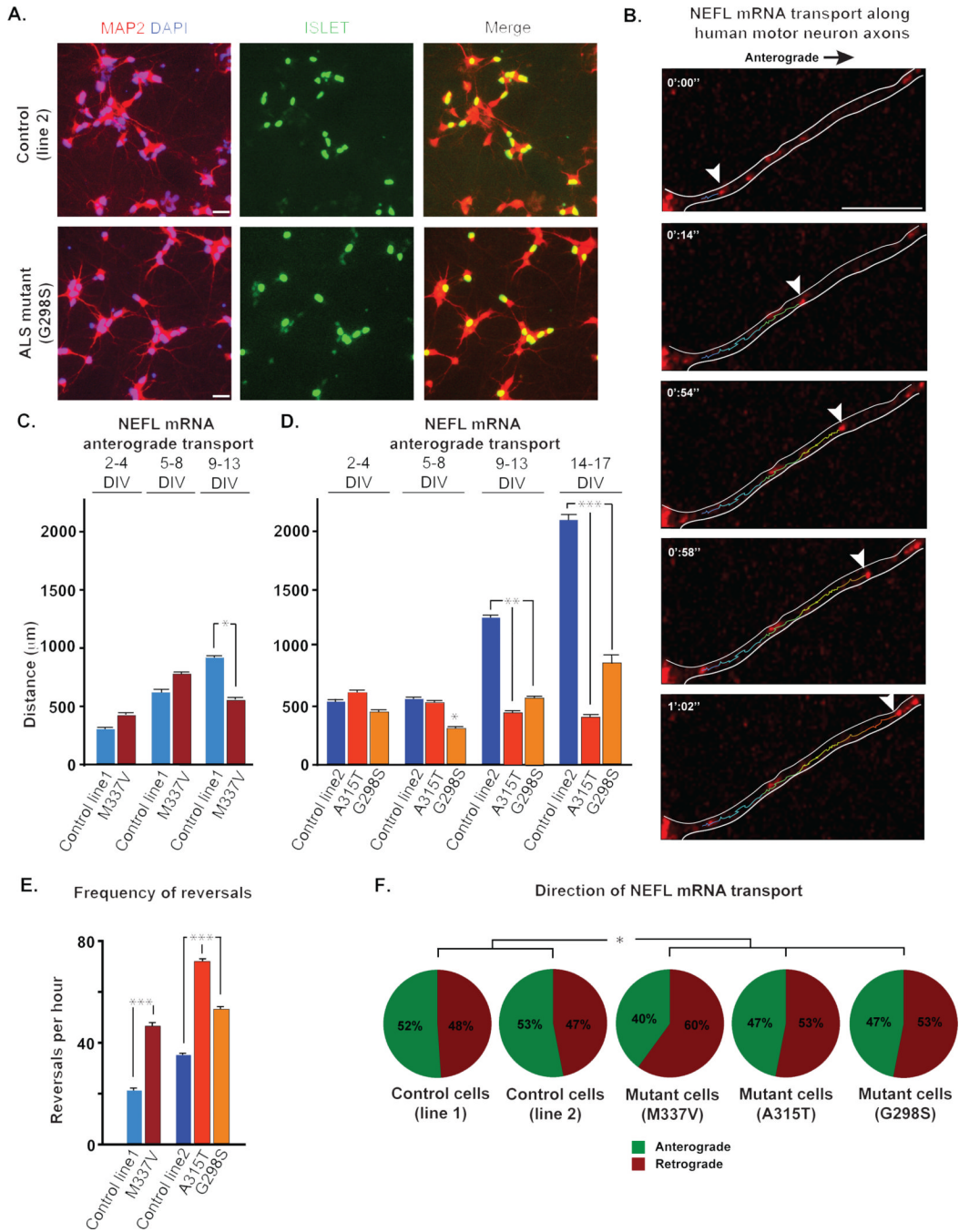


**Fig. 4. NEFL mRNA transport defect along human motor neuron axons**

(A) Human motor neurons were derived from iPS cells, as illustrated with immunostaining for motor neuron markers like Islet. For live imaging, we identified cells based on expression of the HB9 responsive GFP construct. (B) Live imaging of stem cell derived human motor neurons shows endogenous NEFL mRNA transport along axons. Scale bar: 5µm. (C) There is no significant difference in net anterograde displacement of NEFL mRNA granules in control vs. patient motor neurons with TDP-43<sub>M337V</sub> mutation during the first week of observation. The transport defect was apparent 9 days after plating when a significant decrease in net anterograde transport of NEFL mRNA granules is observed. (D) NEFL mRNA anterograde displacement was significantly altered in human motor neurons

from iPS cells of ALS patients with TDP-43<sup>G298S</sup> mutation after 5 days in culture as compared to control. After 9 days in culture, mRNA anterograde transport is significantly altered in motor neurons from all ALS patients as compared to control. This defect becomes more pronounced over time. (E) Frequency of NEFL mRNA granule reversals per hour is significantly higher in neurons with mutant TDP-43 as compared to control, 2 weeks after plating ( $p < 0.001$ ). (F) The percentage of retrogradely moving NEFL mRNA granules is significantly higher in 9 DIV neurons from ALS patients with mutant TDP-43. All error bars are shown as mean  $\pm$  SEM.